



Article

Development of a New HiBiT Biosensor Monitoring Stability of YAP/TAZ Proteins in Cells

Liqing Wu [†], Anni Ge [†], Yawei Hao and Xiaolong Yang ^{*}

Department of Pathology and Molecular Medicine, Queen's University, Kingston, ON K7L 3N6, Canada; yh5@queensu.ca (Y.H.)

* Correspondence: yangx@queensu.ca; Tel.: +1-613533-6000 (ext. 75998)

[†] These authors contributed equally to this work.

Abstract: The Hippo signaling cascade is frequently dysregulated in a variety of cancers, such as breast cancer (BC), which is one of the most commonly diagnosed malignancies in women. Among BC subtypes, triple-negative BC (TNBC) stands out due to its poor prognosis and high metastatic potential. Despite extensive research aimed at establishing treatment options, existing therapies demonstrate limited efficacy for TNBC. Recently, it has been recognized that targeting the core components of the Hippo pathway (YAP and its paralog TAZ) is a promising strategy for developing anti-cancer treatment. However, no YAP/TAZ inhibitors have been approved by the FDA as anti-TNBC treatments, and only a few compounds have been identified that directly affect YAP and TAZ activity and stability to enhance the prospect of innovative HiBiT biosensors for monitoring of YAP and TAZ in cells. Employing these biosensors, we conducted a small-scale drug screen involving 279 compounds, leading to the identification of several small molecule inhibitors (SMIs) capable of inducing YAP/TAZ degradation in diverse TNBC cell lines. It is worth noting that some drugs may indirectly affect the protein stability following prolonged treatment, and a shorter exposure can be included in the future to identify drug candidates with more direct effects. Nevertheless, our study introduces a novel approach for assessing YAP and TAZ levels, which can have significant implications for developing anti-TNBC targeted therapies.



Citation: Wu, L.; Ge, A.; Hao, Y.; Yang, X. Development of a New HiBiT Biosensor Monitoring Stability of YAP/TAZ Proteins in Cells. *Chemosensors* **2023**, *11*, 492. <https://doi.org/10.3390/chemosensors11090492>

Academic Editor: Chunsheng Wu

Received: 10 July 2023

Revised: 25 August 2023

Accepted: 4 September 2023

Published: 6 September 2023



Copyright: © 2023 by the authors. Licensee MDPI, Basel, Switzerland. This article is an open access article distributed under the terms and conditions of the Creative Commons Attribution (CC BY) license (<https://creativecommons.org/licenses/by/4.0/>).

1. Introduction

Cancer remains a leading cause of mortality worldwide, accounting for 10 million deaths in 2020 [1]. Among all cancer cases, breast cancer (BC) is the most common malignancy reported in women [2]. In the year 2022 alone, BC constituted approximately 25% of all newly diagnosed cancer cases, contributing to 14% of the total cancer-related deaths in women [2]. Based on the molecular features of the tumor, BC can be classified into three main subtypes: hormone receptor positive (estrogen receptor (ER+) or progesterone receptor (PR+)), human epidermal growth factor 2 (HER2) positive (HER2+), and TNBC (low or no expression of all three biomarkers) [3,4]. TNBC patients, which accounted for 15% of all breast carcinomas, often displayed high heterogeneity and earlier disease onset [3–5]. Compared to other BC subtypes, TNBC patients exhibited poorer prognoses and more aggressive pathology, with an increased risk of local and distant relapses and metastases [6–8]. Indeed, women diagnosed with TNBC usually experienced an increased possibility of distant recurrence and lower breast-specific survival relative to other types of BC, though the recurrent rate of TNBC decreased dramatically from 4 years after diagnosis [6]. Notably, different factors may predispose patients to certain BC subtypes, including lifestyle, ethnicity, and genetic mutation. Indeed, a higher risk of TNBC was observed among parous women who had several children [7]. TNBC also disproportionately occurred in African American populations with more advanced tumors and higher histologic

and nuclear grade, relative to Caucasian patients [7,9]. Moreover, over 75% of BC patients carrying the *BRCA1* mutation exhibited the TNBC phenotype [5].

Given that TNBC tumors are characterized by a low or absent expression of hormonal receptors and HER2, traditional interventions like endocrine therapy or trastuzumab prove ineffective for these patients [3,5,7,10,11]. Chemotherapy (chemo) has emerged as the standard for treating TNBC, which suppresses tumor growth by facilitating the anti-tumor immune response [3]. Chemo can be administered either as a standalone treatment or in combination with Granulocyte-MQ Colony Stimulating Factor (GM-CSF), yielding a combined therapy that has demonstrated improved clinical outcomes for BC patients [3]. However, when viewed as a group, TNBC patients exhibited worse outcomes after chemo, and diverse responses to chemo had been observed among women with TNBC [5]. Neoadjuvant therapy involving pre-surgical chemo has proven effective predominantly for a subset of TNBC patients, leaving a majority with persistent residual disease post-treatment [5,11]. Despite the varied clinical outcomes after administration, chemo is still the only systemic treatment for TNBC patients [8]. On the other hand, the development of targeted therapeutic agents, such as angiogenesis inhibitor bevacizumab, may benefit women with ER- and PR- BCs [5]. Moreover, the enzyme poly (adenosine diphosphate-ribose) polymerase (PAPR) has garnered attention as a TNBC clinical target due to its involvement in DNA repair mechanisms [5]. While introducing a PAPR inhibitor alongside chemotherapy has shown augmented tumor regression, it has not translated into prolonged overall survival [5]. Furthermore, the responses to targeted agents were diverse, in part due to high heterogeneity among TNBC patients, thereby impeding effective targeted therapy [8]. Consequently, it remains important to explore more BC treatment options with improved efficacy.

The Hippo pathway was initially discovered in *Drosophila* as the regulator of cell growth [12]. Further study revealed that the Hippo signaling pathway is highly conserved in mammals, consisting of the mammalian sterile 20-like kinase (MST), large tumor suppressor (LATS) kinases, scaffold proteins Salvador homolog 1 (SAV1), and Mps One Binder kinase activator protein 1 (MOB1) [13]. In response to extracellular or internal stimuli, such as cell–cell contact and DNA damage, the Hippo signaling pathway is activated. This activation involves phosphorylation of LATS by MST with the assistance of scaffold proteins [14]. The activated LATS induces phosphorylation of the transcriptional coactivators, yes-associated protein (YAP) and its paralog Transcriptional coactivator with PDZ-binding motif (TAZ), promoting their cytoplasmic sequestration and/or proteasomal degradation [15,16]. Conversely, the suppression of this Hippo kinase cascade results in nuclear translocation of YAP and TAZ, enabling them to regulate the expression of their target genes, such as secretory protein connective tissue growth factor (CTGF) and cysteine-rich angiogenic inducer 61 (CYR61) [17–20]. Since YAP and TAZ lack DNA binding domains, they rely on interactions with transcriptional factors such as including transcriptional enhancer associate domain (TEAD) family proteins, RUNX, and SMADs to modulate gene expression [17,18]. TEAD proteins function as the major mediators of YAP/TAZ in regulating gene expression and cell proliferative [21]. Due to interdependence between YAP and TEAD, strong selection pressure has been imposed on both genes, which displayed significant coevolution [22].

Frequent observation of elevated YAP/TAZ nuclear translocation in human cancers stems from disrupted upstream Hippo kinases, resulting in the overactivation of YAP/TAZ, a condition conducive to tumorigenesis [23,24]. In non-tumor BC cells, an overexpression of YAP or TAZ promotes tumorigenic and metastatic processes, such as cell transformation and increased cell migration [25,26]. For instance, YAP overexpression in human non-transformed mammary epithelial cells induced epithelial-to-mesenchymal transition (EMT), triggered an anti-apoptosis response, and facilitated growth factor-independent growth [25]. Similarly, TAZ is an oncprotein that is essential for sustaining self-renewing and neoplastic properties in BC stem cells (BCSCs) [23]. The prognosis of TNBC patients was discovered to be inversely correlated with the expression level of TAZ [27]. In contrast, loss of TAZ expression led to increased cell growth and anchorage-independent growth in soft agar for

184A1 and MCF7 BC cells, respectively [26,28]. Enhanced YAP/TAZ-modulated signals were also responsible for reduced early tumor suppression and TGF- β -mediated tumorigenic phenotypes in the late stage of malignancy [29]. Together, these studies suggest that the Hippo pathway plays an important role in controlling tumor development, and the disruption of YAP/TAZ activity may be a promising route for generating efficient BC therapy.

To specifically monitor the protein of interest, bioluminescence methodologies have been frequently exploited in a non-invasive manner [30]. The discovery of the luciferase enzyme has paved the way for establishing a diverse array of biochemical assays [31–33]. While firefly and Renilla luciferases are commonly utilized for assessing the biological activities of target proteins, NanoLuc—a small, bright, and stable luciferase originating from deep-sea shrimp *Ophophorus gracilirostris*—has been discovered and developed into complementary assays, which effectively detect protein–protein interactions (PPIs) and protein activity [34–37]. Referred to as the split NanoLuc luciferase reporter system, the NanoLuc complementary assay comprises two subunits: large N-terminal BiT (LgBiT; 17.6 kDa) and small C-terminal BiT (SmBiT; 1.3 kDa) [38]. The bright luminescence was detected in the presence of its substrate furimazine when the two subunits of NanoLuc (LgBiT and SmBiT) were brought together by PPIs [38]. Recently, a novel subunit, HiBiT, which is mutated from SmBiT, has been engineered to possess an exceptionally higher affinity to LgBiT, compared to the original SmBiT [39]. To use this system for quantifying protein expression levels, the HiBiT tag is first fused with a gene of interest (GOI). The resultant HiBiT-GOI fusion proteins or protein lysates expressing HiBiT-GOI are mixed with purified LgBiT. Because of the strong affinity between HiBiT and LgBiT, an active NanoLuc is generated in tandem, emitting a brilliant luminescent signal upon the introduction of its substrate [39]. The intensity of these bioluminescent signals is believed to respond to the quantities of HiBiT-GOI protein being expressed. Therefore, this HiBiT system can be used for monitoring protein levels both *in vivo* and *in vitro*.

In this research, we applied the split NanoLuc technology and generated HiBiT-tagged YAP and TAZ proteins to monitor their stability in cells (Figure 1a). After the HiBiT bioluminescent biosensors were validated *in vitro* and *in vivo*, we subjected the optimized HiBiT biosensors to a small-scale drug screening with two libraries of 279 compounds for identifying SMIs that could degrade YAP and TAZ in TNBC cells. Multiple candidates were identified to inhibit the stability of YAP and TAZ *in vivo*. Our data show that our established HiBiT biosensors display great potential in monitoring YAP/TAZ stability, which is an encouraging strategy to discover targeted therapies for TNBC treatment.

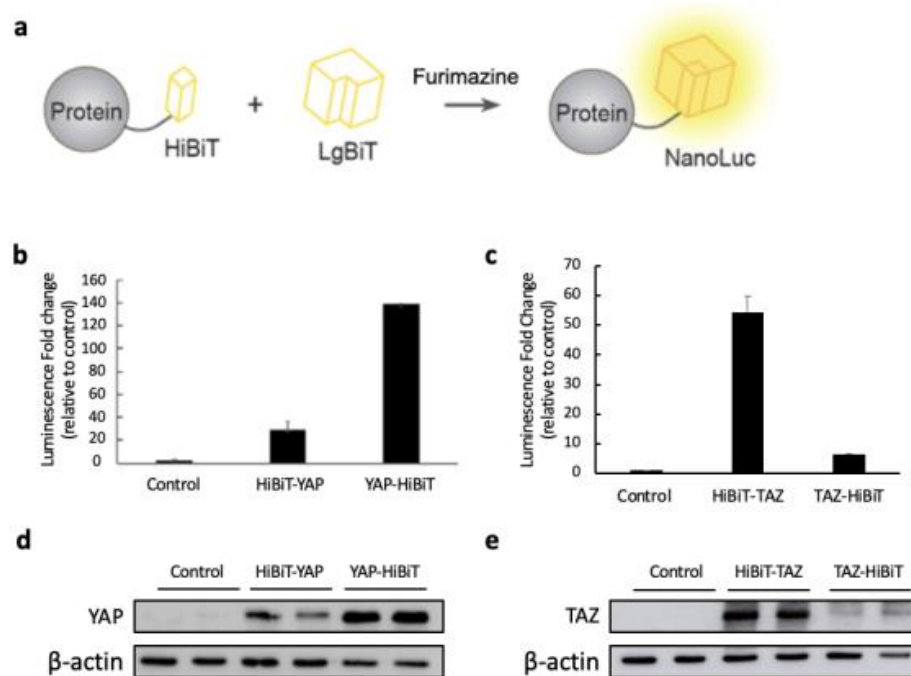


Figure 1. Establishing HiBiT-tagged YAP and TAZ biosensors monitoring protein stability. (a) Schematic representation of the HiBiT biosensors for detecting the YAP and TAZ protein levels. (b,c) The HiBiT sequence was attached at either the N- or C-terminus of YAP and TAZ, and each construct was subcloned into the pcDNA3.1-3xFLAG vector. These plasmids were individually transfected into the HEK293 cells in the 12-well plate. The empty pcDNA3.1 vector was transfected into the cells as a negative control. After 48 h post-transfection, protein lysates were extracted with 1× passive lysis buffer (PLB). The luciferase assay was performed by combining 2.5 µg of each lysate and 0.5 µg of purified LgBiT-His protein. The mixture was then incubated before the addition of the substrate. The luminescent fold change was determined by calculating how much the bioluminescence from the HiBiT biosensor increased compared to the empty vector control after the addition of LgBiT-His protein and NanoLuc substrate. The data are shown as mean + SD ($n = 2$ technical replicates) (d,e) The expression level of each construct was examined by WB using 10 µg of each cell lysate. β-actin was detected as the internal loading control.

2. Materials and Methods

2.1. Cell Culture

MDA-MB-231 (human mammary carcinoma), HEK293 (human embryonic kidney cells), and HEK293T (human embryonic kidney cells) cells were cultured in Dulbecco's Modified Eagle's Medium (DMEM; Sigma#D6429, Oakville, ON, Canada) containing 10% fetal bovine serum (FBS) and 1% penicillin/streptomycin (P/S) (Invitrogen, Burlington, ON, Canada). BT-549 (human mammary carcinoma) cells were cultured in RPMI-1640 Medium (Sigma #8758) containing 10% FBS, 1% P/S, and 0.023 U/mL of insulin. MDA-MB-231 with YAP and TAZ knockout (KO) were established as described [40] and cultured in the same medium as previously mentioned. All cells were kept at 37 °C with 5% CO₂.

2.2. Plasmid Construction

HiBiT-tagged full-length (FL) YAP and TAZ were prepared by amplifying the FL YAP and TAZ genes using PCR from cDNA and inserting into the pcDNA3.1 vector with either N- or C-terminal HiBiT (sequence: VSGWRLFKKIS). Plasmids for producing GST fusion proteins were constructed by cloning LgBiT into the BamHI/NotI sites of pGEX-4T1 vector. See supporting information for primers used in cloning (Table S1).

2.3. LgBiT Protein Purification from Bacteria

The BL21 *Escherichia coli* strain was transformed and utilized to purify LgBiT-His fusion protein according to the previously established protocols with minor adjustments in our lab [41]. After inoculation, when the OD₆₀₀ reached 0.7–0.9, protein expression was induced with 0.4 mM of IPTG (isopropyl β-D-1 thiogalactopyranoside) at 37 °C incubation for 4–5 h. Bacterial cells were spun down, washed, and lysed by sonication. His-LgBiT fusion proteins were purified by Ni-NTA beads, visualized, and quantified with BSA by SDS-PAGE and Coomassie blue staining. The purified protein was stored at –80 °C.

2.4. Protein Extraction and Western Blot Analysis

Cells were cultured to 80–90% confluence before protein extraction. Either RIPA (50 mM of Tris HCl, 150 mM of NaCl, 1.0% (v/v) NP-40, 0.5% (w/v) Sodium Deoxycholate, 1.0 mM of EDTA, 0.1% (w/v) SDS, and 0.01% (w/v) sodium azide, pH = 7.4) with the complete EDTA-free protease inhibitor cocktail tablet (Roche, Mississauga, ON, Canada) or 1× passive lysis buffer (PLB) (Promega, Madison, WI, USA) was utilized to lyse the cells. The cell lysates were collected and centrifuged at 12,000 × g at 4 °C for 10 min to obtain the supernatant, and the DC protein assay kit (Bio-Rad, Mississauga, ON, Canada) was used to measure the protein concentration. The protein expression levels were analyzed by Western blot (WB) using 10–30 µg of protein lysates for each sample, which was boiled with 5× loading buffer (4.2% β-Mercaptoethanol) at 95 °C for 5 min. SDS-PAGE (10–12%) was performed to resolve the proteins, which were transferred to nitrocellular membrane (Bio-Rad, Mississauga, ON, Canada). TBST buffer ((20 mM of Tris, 150 mM of NaCl, 0.1% Tween 20) containing 5% skimmed milk was used to block the membranes for one hour at room temperature. The blocked membranes were probed with primary antibodies at 4 °C overnight or for 1 h at room temperature and washed with TBST buffer before probing with secondary antibodies (1:4000 dilution) for 15 min at room temperature. The protein bands were visualized by chemiluminescence reagent (Bio-Rad). The antibodies were stripped with stripping buffer and re-probed with anti- β-actin antibody. The antibodies and corresponding dilutions are as follows: mouse monoclonal anti-FLAG (F1804, Sigma, 1:1000) antibody; rabbit polyclonal anti-YAP (sc-15407, Santa Cruz, Dallas, TX, USA, H125, 1:1000); mouse monoclonal anti-TAZ (560235, BD Biosciences, Mississauga, ON, Canada, 1:1000); mouse monoclonal anti-β-actin (A5441, Sigma, 1:1000).

2.5. NanoGlo Luciferase Assay

Purified His-LgBiT protein and cell lysates expressing HiBiT-tagged YAP or TAZ were mixed and incubated for at least 10 min on ice before measuring the luminescence with 1:50 diluted Nano-Glo Live Reagent (Promega) using GloMax Navigator Detection System (Promega).

2.6. Small-Scale Drug Screen

The drug screening with 279 compounds was performed using bioactive lipid and custom compound libraries. The experimental conditions were as follows. The MDA-MB-231 cells with YAP and TAZ KO were either transfected with the plasmid expressing YAP-HiBiT or HiBiT-TAZ in the 6-well plate. After 5 h post-transfection, the cells were trypsinized and counted for seeding into the 96-well plates with 40–50% confluency the next day. The cells were then treated with the drug candidates at a concentration of 100 µM for 48 h. After that, the bioluminescence and cell viability were measured and compared against the 1% DMSO-treated control samples for calculating the fold changes. A complete list of drug candidates can be seen in Table S2.

2.7. Cell Viability Assay

After treating the transfected YAP and TAZ KO MDA-MB-231 cells with different drugs, the plates and the contents were equilibrated to room temperature for approximately 30 min. A volume of CellTiter-Glo 2.0 Reagent (Promega) equal to the volume of cell culture

medium per well was added and mixed for 2 min on an orbital shaker to induce cell lysis. The plate was then incubated for 10 min before examining the luminescent signal using GloMax Navigator Detection System (Promega).

2.8. Densitometric Analysis by ImageJ

After the MDA-MB-231 cells were treated with either of the 67 initial hits, cell lysates were extracted using RIPA buffer and used for WB. For protein band quantitation, the WB images were analyzed using the Gel Analyzer tool of ImageJ (NIH, Version 1.53t). The band intensity was measured for YAP, TAZ, and β -actin (loading control) and subjected to background subtraction to calculate the net signal. The protein expression for each band was normalized by determining the ratio of a net band signal over the net loading control of that lane. The YAP and TAZ expression ratios of the drug-treated samples were reported by comparing with the DMSO-treated controls (Table S4).

2.9. RNA Extraction and Quantitative Real-Time PCR

MDA-MB-231 cells were seeded in 6-well plates with 50–60% confluence the next day and then treated with either avanafil (100 μ M), beta-carotene (20 μ M), dipyridamole (50 μ M), fluvastatin (10 μ M), pterostilbene (100 μ M), or XEN445 (100 μ M). 48 h post-treatment, RNA was extracted using RNAZol RT reagent (200 μ L/well) based on the manufacturer's instruction. A quantitative real-time PCR (qRT-PCR) was performed using 50 ng of RNA/reaction by the SuperScript III Platinum SYBR Green One-Step qRT-PCR Kit (Invitrogen). The 18S rRNA was measured as an internal control.

2.10. Statistical Analysis

For all figures, data are shown as mean + or \pm SD. An ANOVA and a Student's *t*-test (two-tailed) were performed for the statistical analysis. A *p*-value < 0.05 was considered statistically significant.

3. Results

3.1. Design and Establishment of HiBiT Biosensors

To monitor the stability of YAP/TAZ, we established the YAP/TAZ-HiBiT biosensors in which a HiBiT peptide was fused with the N or C-terminus of a YAP or TAZ protein. The YAP/TAZ-HiBiT was expected to have a high affinity to LgBiT, forming an active NanoLuc, which could emit strong bioluminescence in the presence of its substrate furimazine (Figure 1a). HEK293T cells were transfected with the plasmids expressing either of the constructs or with an empty pcDNA3.1 vector as a negative control.

The luminescence of each HiBiT biosensor was measured by luciferase assays using purified His-tagged LgBiT from bacteria and cell lysates containing HiBiT-tagged YAP/TAZ. The combination of His-LgBiT and HiBiT-tagged YAP/TAZ displayed high luminescent increases compared to the negative control (Figure 1b,c). Interestingly, attaching the HiBiT tag to the C-terminus of YAP resulted in a stronger luminescent signal, while higher luminescence was observed when the HiBiT tag was fused to the N-terminus of TAZ (Figure 1b,c). The protein levels of the HiBiT-tagged YAP/TAZ were detected by Western blot, suggesting that the high bioluminescence of YAP-HiBiT and HiBiT-TAZ resulted from the high protein overexpression in transfected cells (Figure 1d,e).

To confirm that the substantial bioluminescent increase indeed resulted from HiBiT and LgBiT fusion protein complementation, two controls were generated by transfecting either the empty pcDNA3.1 vector or the plasmid expressing FLAG-YAP/TAZ into HEK293T cells. High protein expression of YAP/TAZ was observed in transfected cells with FLAG-YAP/TAZ or HiBiT-YAP/TAZ-expressing plasmids, whereas low protein levels were detected in the empty vector control (Figure 2a). However, the strong bioluminescent signals were only exhibited in cells transfected with HiBiT biosensor-expressing plasmids (Figure 2b). Our data indicate that the HiBiT BS were established and optimized by fusing the HiBiT to the C-terminus of YAP and the N-terminus of TAZ, which emitted

strong bioluminescence after the complementation with LgBiT-His and could be useful for monitoring protein stability.

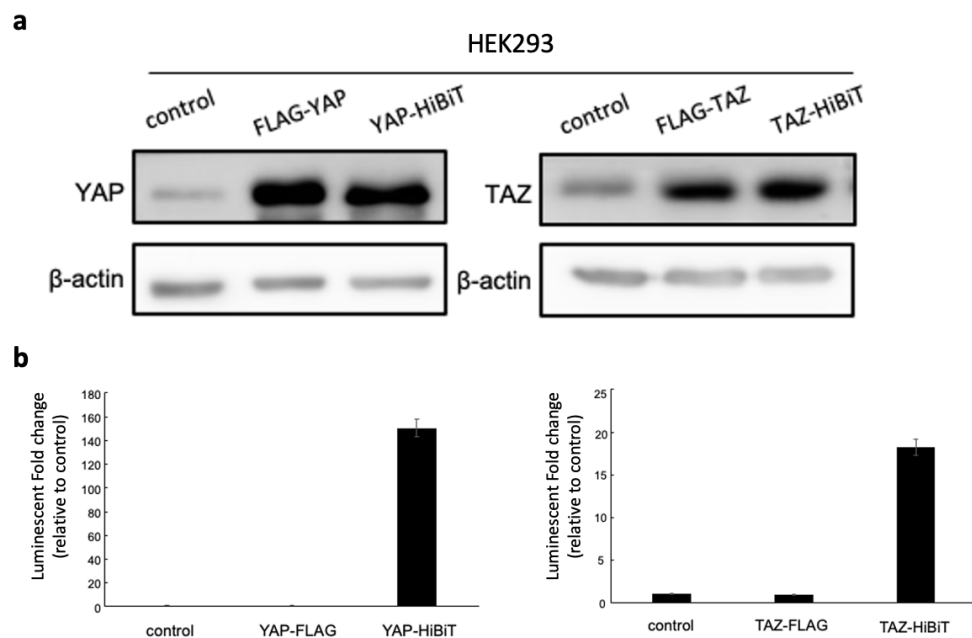


Figure 2. (a) The protein expression of HiBiT-tagged YAP/TAZ in mammalian cells. The HEK293 cells were either transfected with pcDNA3.1 empty vector as the control, FLAG-YAP/TAZ or HiBiT-YAP/TAZ expressing plasmids. Forty-eight hours post-transfection, cells were lysed using RIPA buffer, and 10 μ g of each lysate was used for detecting YAP/TAZ levels by WB. Lysates from cells transfected with empty vector and FLAG-YAP/TAZ-expressing plasmids were included as negative and positive controls for YAP/TAZ expression. The expression of β -actin was detected as an internal control. (b) After the protein extraction, 5 μ g of each cell lysate was combined with 1 μ g of LgBiT-His protein purified from *Escherichia coli*. The mixture was incubated for 10 min before adding NanoGlo substrate for luminescent measurement. The relative luminescence of each lysate was normalized to the signal from the empty vector control to calculate the fold increase. Substantial luminescence was found exclusively in HiBiT biosensors. The data are represented as the mean + SD ($n = 3$ technical replicates).

3.2. Validation of HiBiT-Tagged YAP/TAZ Biosensor

Next, we sought to validate the HiBiT biosensors by in vitro luciferase assays. An increasing amount of plasmids expressing the optimized HiBiT-tagged biosensors was transfected into HEK293T cells. As expected, the bioluminescent signals increased as the cells were transfected with more plasmids, demonstrating that only 0.5 μ g of plasmids was sufficient to produce strong luminescent signals (Figure 3a,c). An elevated expression level of YAP-HiBiT or HiBiT-TAZ coincided with the increased amount of plasmid used for transfection (Figure 3b,d). Moreover, a linear relationship was observed between the luminescent intensity and the number of transfected cells subjected to bioluminescent analysis (Figure 3e,f). These results suggest that the luminescent intensity of HiBiT biosensors was affected by the expression levels of HiBiT-tagged YAP/TAZ, indicating that our stable HiBiT biosensors could be applied for drug screening.

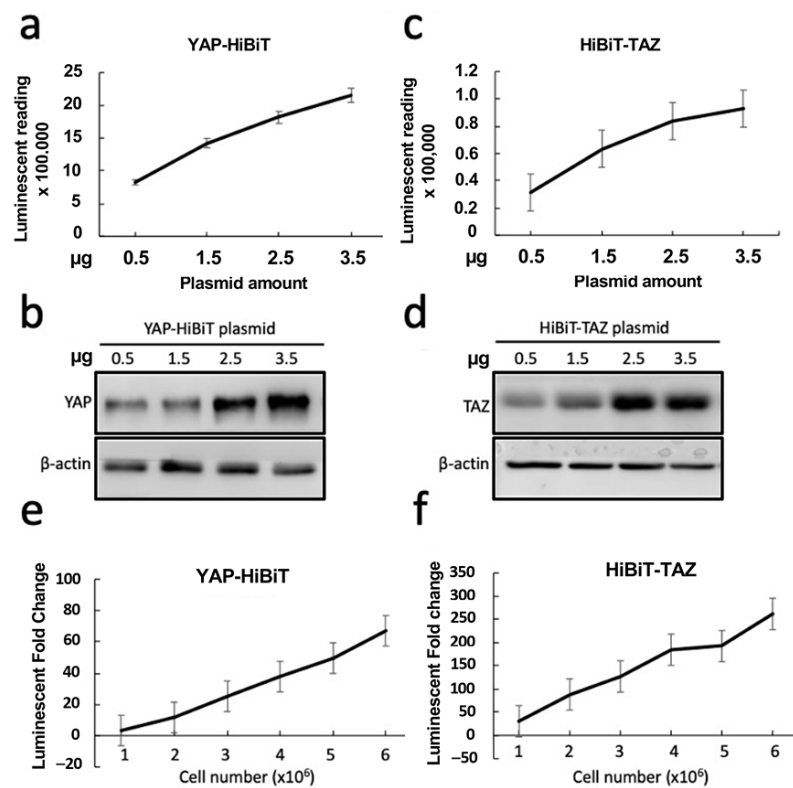


Figure 3. Validation of HiBiT BSs. (a–d) The plasmids expressing YAP-HiBiT or HiBiT-TAZ were transfected into the HEK293 cells in increasing amounts. After 48 h post-transfection, the cells were lysed with 1× PLB and subjected to luciferase assays ($n = 4$ biological replicates) (a,c) and WB (b,d) to compare the HiBiT BS activity and protein expression. (e,f) Detection of luminescent signal with increasing numbers of transfected HEK293 cells ($n = 4$ biological replicates). The cells were transfected with YAP-HiBiT- or HiBiT-TAZ-expressing plasmids in a six-well plate. After 48 h post-transfection, the transfected cells were counted and seeded into each well of a 96-well plate with increasing cell numbers, as indicated in the x-axis. The luciferase activity of each well was measured 16 h later. All bioluminescent data are represented as mean \pm SD.

After we confirmed that the luminescent intensity was dependent on the protein levels of HiBiT-tagged YAP/TAZ, the HiBiT biosensors were further validated by a known YAP/TAZ inhibitor, docosahexaenoic acid (DHA), which was reported to affect the protein levels of YAP and TAZ [42]. The HEK293T cells transfected with either YAP-HiBiT or HiBiT-TAZ-expressing plasmids were treated with DHA over 4 days. The protein lysates were obtained at 0, 0.5, 1-, 2-, 3-, and 4-days post-treatment, followed by WB. Since the literature had discovered that DHA could reduce the level of β-actin in cells [43], ponceau S staining was shown instead as an indicator of equal protein loading for WB. Decreased HiBiT-tagged YAP and TAZ expression was detected by WB in a time-dependent manner after treatment (Figure 4a,b). This reduced expression of YAP/TAZ was not due to the degradation of the HiBiT tag by DHA because DHA also reduced endogenous YAP/TAZ (Figure S1), as previously reported [42]. Next, we examined the luciferase activity using the same lysates at later time points, as the most prominent changes in YAP/TAZ stability were observed after 3 and 4 days of DHA treatment. Indeed, significant reductions in the bioluminescent signal were observed on days 3 and 4 post-treatment, compared to the luminescence at day 0 (Figure 4d,e). Furthermore, to ensure that the reduced bioluminescence was not due to the direct HiBiT degradation, a control was created by directly fusing the HiBiT sequence to the C-terminus of LgBiT. The HEK293T cells transfected with LgBiT-HiBiT-expressing plasmids were treated with DHA using the same condition. Unlike previous results, DHA did not reduce the stability of LgBiT-HiBiT and its bioluminescence after prolonged treatment (Figure 4c,f). Taken together, these results demonstrate the high

specificity of our HiBiT biosensors in monitoring the stability of YAP and TAZ and show that the HiBiT biosensors are applicable for the drug screening campaign to identify drugs that induce YAP/TAZ degradation.

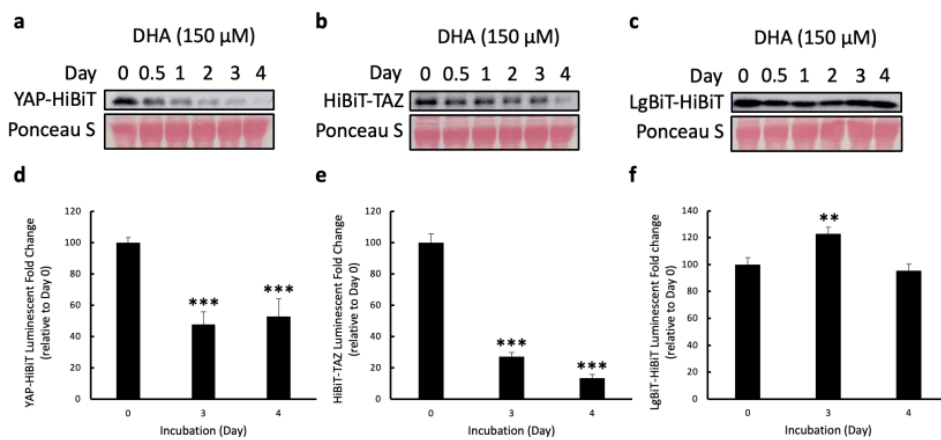


Figure 4. Validation of HiBiT BS with a known YAP/TAZ inhibitor, DHA. (a–c) The HEK293T cells were transfected with either HiBiT-TAZ-, YAP-HiBiT-, or LgBiT-HiBiT-expressing plasmids. After 5 h post-transfection, each transfected cell line was counted, and triplicates of 2×10^5 cells/well for each cell line were seeded into the 12-well plates. The next day, the cells were treated with 150 μ M of DHA. The stability of YAP-HiBiT (a), HiBiT-TAZ (b), and LgBiT-HiBiT (c) was examined by WB with 10 μ g of cell lysates at 0, 0.5, 1, 2, 3, 4 days post-treatment. Ponceau S staining was shown as the loading control. (d–f) The luciferase assays were conducted using 2.5 μ g of each cell lysate at 0-, 3-, and 4-days post-treatment to assess the prolonged effect of DHA in YAP and TAZ stability. The luminescent fold change was measured by calculating how much the bioluminescence from the treated lysates changed relative to the luminescent signal at day 0 of treatment. The data are presented as mean + SD 2 independent experiments, ** $p < 0.01$, *** $p < 0.001$.

3.3. Identification and Validation of SMIs Targeting HiBiT-Tagged YAP/TAZ Biosensors in TNBC Cells

A small-scale drug screen with two libraries consisting of 279 small molecules, including the bioactive lipid library and custom compound library, was conducted using our validated HiBiT biosensors to find drugs that could degrade YAP and TAZ in TNBC cells. The YAP and TAZ KO MDA-MB231 cells expressing YAP-HiBiT or HiBiT-TAZ were treated with each drug from the libraries. The luminescence and cell viability were determined after 48 h post-treatment. After excluding the compounds that were too toxic for the cells (cell viability fold change < 0.2), a total of 67 compounds that displayed notable HiBiT signal fold changes (< 0.5 or > 1.8) were selected as the initial hit candidates for subsequent validations (Figure S2).

To explore the effect of the initial hits on YAP/TAZ stability, these drugs were used to treat MDA-MB-231 cells for assessing the endogenous levels of YAP and TAZ by WB after 48 h of treatment. Relative to DMSO controls, 22 out of 67 candidates greatly reduced the expression of both YAP and TAZ (expression ratio < 0.4), while eight additional drugs seemed to preferentially inhibit TAZ protein level (Figure 5; Table S4). To further verify the impact of those candidates on YAP/TAZ stability, MDA-MB-231 cells were treated with these drugs again to determine the expression levels of YAP and TAZ at different times post-treatment. Finally, six drugs were found to decrease the endogenous levels of YAP/TAZ in a time-dependent manner, including small molecules from plant extracts (pterostilbene and beta-carotene), lipid-related (fluvastatin and XEN445), and phosphodiesterase (PDE) inhibitors (avanafil and dipyridamole) (Figure 6a–f).

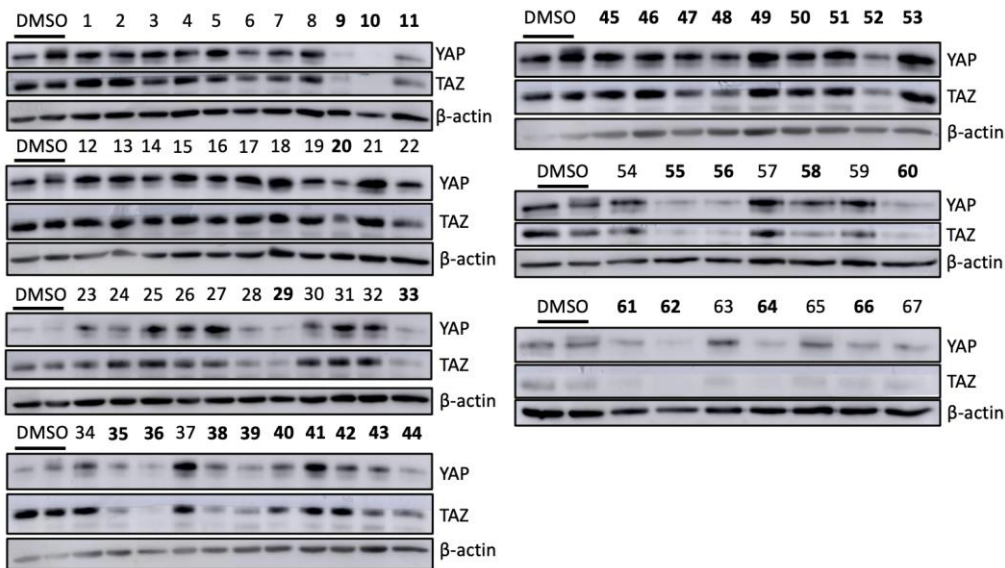


Figure 5. The effect of initial hit candidates on endogenous levels of YAP/TAZ in the TNBC cells. MDA-MB-231 cells were treated with 100 μ M of 67 initial hits separately for 48 h. To compare the YAP and TAZ stability after each treatment, cells cultured with only DMSO were included as controls. Cell lysates were harvested using RIPA buffer and used for WB to assess the protein levels of YAP and TAZ. Among the initial 67 candidates, 22 compounds affected the YAP and TAZ stability in TNBC cells, and TAZ expression was specifically inhibited by additional eight drugs. The bolded numbers indicated that the corresponding drugs decreased the protein levels of both YAP and TAZ or preferentially inhibited TAZ expression.

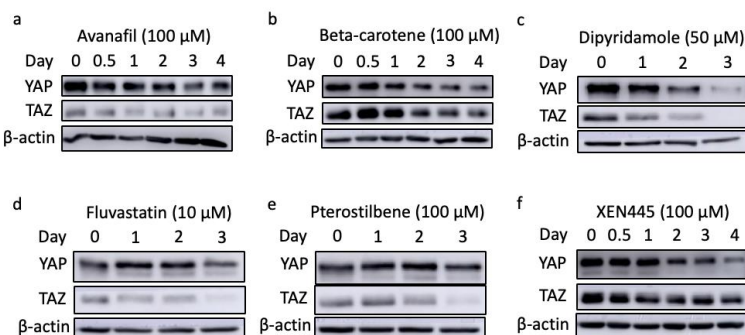


Figure 6. The YAP/TAZ stability in MDA-MB-231 cells treated with top candidates, including avanafil (a), beta-carotene (b), dipyridamole (c), fluvastatin (d), pterostilbene (e), and XEN445 (f).

To examine whether the loss of YAP/TAZ expression was due to a reduction in mRNA level rather than protein degradation, RNA was extracted from MDA-MB-231 cells that were pre-treated with either of the six candidates for 48 h. Based on our results, all of the drugs had no considerable inhibitory impact on the mRNA levels of YAP and TAZ (Figure 7). In addition, four out of the six top candidates significantly increased the level of TAZ mRNA relative to DMSO-treated controls (Figure 7). Moreover, another TNBC cell line, BT-549, was treated with the identified six drugs along with a known inhibitor, DHA, to avoid any cell line-specific effect. Consistent with our previous findings, reduced YAP and TAZ protein levels were observed in the treated cells relative to the control (Figure 8). Altogether, these data reveal multiple small molecules that affected the stability of YAP and TAZ in TNBC cells through drug screening using our HiBiT biosensors. Hence, the use of HiBiT biosensors exerts great potential for assessing the levels of YAP and TAZ proteins in vivo and identifying pre-existing compounds that regulate the stability of YAP and TAZ.

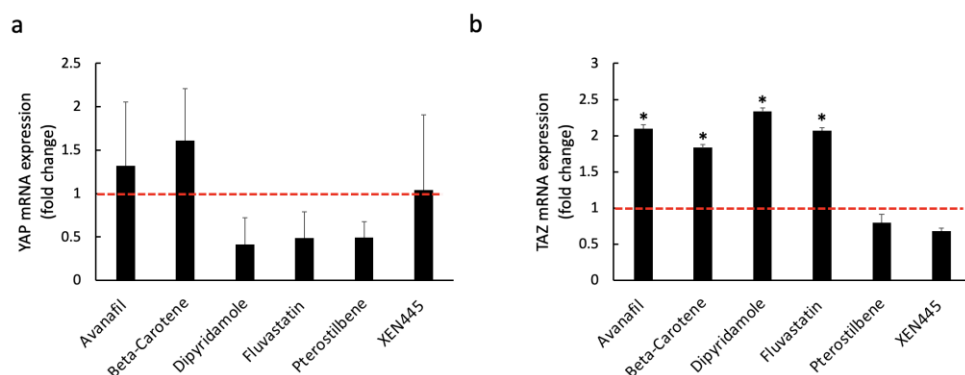


Figure 7. The mRNA levels of YAP (a) and TAZ (b) in MDA-MB-231 cells treated with either avanafil (100 μ M), beta-carotene (20 μ M), dipyridamole (50 μ M), fluvastatin (10 μ M), pterostilbene (100 μ M), or XEN445 (100 μ M). After 48 h post-treatment, RNA was extracted using RNAzol RT, and RT-qPCR was performed to assess the mRNA levels of YAP and TAZ. The cells treated with 1% DMSO for two days were included as the control. The mRNA expression fold change was calculated by measuring the difference between drug-treated and DMSO-treated samples. Based on ANOVA analysis of our data, the mRNA expression of YAP and TAZ is not significantly inhibited ($p \geq 0.05$) by either of the drugs in MDA-MB-231 (qRT-PCR; mean + SD, $n = 2$ biological replicates (2 replicates for each biological sample), t -test: * $p < 0.05$).

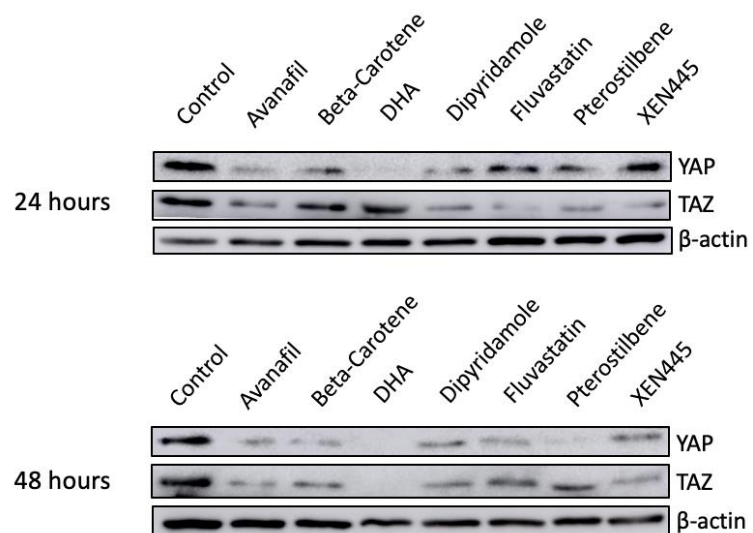


Figure 8. Validation of top candidates in BT549. Seven drugs, including avanafil (100 μ M), beta-carotene (20 μ M), DHA (150 μ M), dipyridamole (50 μ M), fluvastatin (10 μ M), pterostilbene (100 μ M), and XEN445 (100 μ M), were used to treat another TNBC cell line to avoid cell line-specific effects. The protein lysate was collected every 24 h for a total of 2 days using RIPA buffer, and 10–30 μ g of each lysate was subjected to WB. Cells treated with 1% of DMSO were included as the negative control.

4. Discussion

BC accounted for approximately 25% of all cancer cases among Canadian women in 2022 [2]. One of the BC subtypes is TNBC, which is characterized by high heterogeneity and low overall survival [7,8]. The existing medical interventions have yielded limited enhancements in the health of those affected, particularly among women diagnosed with TNBC. Adding to this challenge, TNBC patients lacking or expressing low levels of hormonal receptors and HER2, remain ineligible for the benefits of most targeted therapy drugs [3,5,7,10,11,44]. Alternatively, emerging novel therapeutics such as molecular-targeted therapy may exhibit significant efficiency in treating women with BCs [3]. Manipulating critical signaling pathways that underlie cancer progression presents

a viable strategy for crafting highly targeted treatments. A pertinent example is the Hippo pathway, which is crucial not only in normal physiological functions, but also in tumorigenesis [14,43,45]. In BC cells, YAP and TAZ are often overexpressed to facilitate disease progression [23–26]. Consequently, targeting YAP and TAZ has emerged as a promising avenue for developing anti-cancer therapy. Many studies are centered around evaluating the dynamics of YAP/TAZ-TEAD interaction [17,18,21]. Currently, three drugs targeting YAP/TAZ-TEAD interaction are undergoing phase I clinical trials, along with an antisense oligonucleotide targeting YAP1 that completes the phase I clinical trial [46–49]. However, less attention is devoted to assessing the stability of YAP and TAZ, despite their potential susceptibility to degradation for developing anti-tumor treatment.

In this study, we have developed novel ultra-stable HiBiT biosensors for monitoring the levels of YAP and TAZ in cells. These differ from the conventional split NanoLuc assay that depends on the interaction of target proteins for the complementation of the SmBiT and LgBiT fragments, which do not spontaneously interact with each other [50]. Many studies have exploited this conventional approach to monitor the activity of YAP/TAZ and their binding partners, mainly TEAD [51]. Although several small molecule disruptors of YAP-TEAD PPI have been identified, most drugs indirectly regulate YAP/TAZ activity by inhibiting autopalmitoylation of TEAD, which affects protein stability [51]. To date, no small molecules have been discovered to exert a direct effect on both YAP and TAZ expression levels. Alternatively, relying on the remarkably high affinity of HiBiT to LgBiT, the levels of YAP and TAZ can be readily detected by our HiBiT biosensors through luminescent analysis upon the addition of LgBiT and their substrate. Two libraries of 276 small molecule compounds were screened using these HiBiT biosensors for identifying potential inhibitors that could degrade YAP/TAZ in TNBC cells. After validation, we uncovered six drugs, including pterostilbene, fluvastatin, beta-carotene, Avanafil, XEN445, and dipyridamole, which significantly reduced the levels of YAP and TAZ in cells.

One of the identified drugs from the screening was pterostilbene (*trans*-3,5-dimethoxy-4'-hydroxystilbene), which was already revealed to suppress the growth of TNBC tumors by facilitating the activation of extracellular signal-regulated kinase (ERK) 1/2 [52,53]. However, the link of this chemical to the Hippo pathway remains elusive. Our results indicate that pterostilbene can induce the degradation of downstream Hippo transducers, YAP and TAZ, although the mechanistic details require further study. Other positive hits, such as avanafil and dipyridamole, are different PDE inhibitors [54,55]. The former is frequently utilized to treat erectile dysfunction and pulmonary arterial hypertension, and dipyridamole is often prescribed for ischemic disorders [54,55]. Tumor-suppressive effects were observed in xenograft mice bearing TNBC cells treated with dipyridamole [55]. Moreover, accelerated YAP phosphorylation and inactivation can be driven by fluvastatin, which is administered for hypercholesterolemia treatment and cardiovascular disease prevention [56]. A potent and selective endothelial lipase inhibitor, XEN445, which increased plasma HDL-cholesterol concentration in mice, was also discovered in our screen [57]. While no connection is found between XEN445 and cancer therapy, there is evidence that relates lipid signaling to the Hippo pathway [58].

Due to the nature of our HiBiT biosensors, potential caveats may occur, and the major limitation of our study is that the degradation of YAP/TAZ after 48 h of treatment may be indirectly caused by drugs. Thus, a shorter treatment may be needed to identify more candidate drugs, exerting a direct effect on YAP/TAZ stability.

In summary, we have shown that our newly developed HiBiT biosensors hold substantial values in investigating the YAP/TAZ levels in cells. By applying the HiBiT biosensors, the drug screening is easily performed to identify pre-existing compounds affecting the stability of YAP/TAZ, which are key targets for anti-tumor therapy. Since no drugs targeting YAP and TAZ have been approved by FDA for TNBC treatment, our data reveal the powerful capability of HiBiT biosensors in the discovery of YAP/TAZ inhibitors to increase the likelihood of finding a successful targeted therapy for TNBC patients.

Supplementary Materials: The following supporting information can be downloaded at: <https://www.mdpi.com/article/10.3390/chemosensors11090492/s1>, Figure S1: Degradation of endogenous YAP/TAZ after DHA treatment; Figure S2: Small-scale screening of YAP/TAZ inhibitors with a bioactive lipid library and custom compound library; Table S1: List of primers for cloning; Table S2: List of bioactive lipid library for small-scale screen; Table S3: List of custom compound library for small-scale screen; Table S4: Quantitation of YAP and TAZ protein levels in TNBC cells treated with either of the initial hits by densitometric analysis.

Author Contributions: Conceptualization, methodology, investigation, L.W., A.G., Y.H. and X.Y.; writing—original draft preparation and editing, A.G.; supervision, project administration, and funding acquisition, X.Y. All authors have read and agreed to the published version of the manuscript.

Funding: This work was supported by grants from Canadian Institute of Health Research (CIHR) (grant number: 148629 and 186142) and Canadian Cancer Society (CCS)/Canadian Breast Cancer Foundation (CBCF) (grant number: 369676).

Institutional Review Board Statement: Not applicable.

Informed Consent Statement: Not applicable.

Data Availability Statement: Not applicable.

Acknowledgments: We would like to thank Dongsheng Tu in his help in our statistical analysis.

Conflicts of Interest: The authors declare no conflict of interest.

References

1. Cancer. Available online: <https://www.who.int/news-room/fact-sheets/detail/cancer> (accessed on 19 December 2022).
2. Canadian Cancer Society. Available online: <https://cancer.ca/en/cancer-information/cancer-types/breast/statistics> (accessed on 19 December 2022).
3. Barzaman, K.; Karami, J.; Zarei, Z.; Hosseinzadeh, A.; Kazemi, M.H.; Moradi-Kalbolandi, S.; Safari, E.; Farahmand, L. Breast cancer: Biology, biomarkers, and treatments. *Int. Immunopharmacol.* **2020**, *84*, 106535. [[CrossRef](#)] [[PubMed](#)]
4. Waks, A.G.; Winer, E.P. Breast Cancer Treatment: A Review. *JAMA* **2019**, *321*, 288–300. [[CrossRef](#)] [[PubMed](#)]
5. Foulkes, W.D.; Smith, I.E.; Reis-Filho, J.S. Triple-negative breast cancer. *N. Engl. J. Med.* **2010**, *363*, 1938–1948. [[CrossRef](#)] [[PubMed](#)]
6. Dent, R.; Trudeau, M.; Pritchard, K.I.; Hanna, W.M.; Kahn, H.K.; Sawka, C.A.; Lickley, L.A.; Rawlinson, E.; Sun, P.; Narod, S.A. Triple-negative breast cancer: Clinical features and patterns of recurrence. *Clin. Cancer Res.* **2007**, *13*, 4429–4434. [[CrossRef](#)] [[PubMed](#)]
7. Phipps, A.I.; Chlebowski, R.T.; Prentice, R.; Tiernan, A.M.; Wactawski-Wende, J.; Kuller, L.H.; Adams-Campbell, L.L.; Lane, D.; Stefanick, M.L.; Vitolins, M.; et al. Reproductive history and oral contraceptive use in relation to risk of triple-negative breast cancer. *J. Natl. Cancer Inst.* **2011**, *103*, 470–477. [[CrossRef](#)]
8. Collignon, J.; Lousberg, L.; Schroeder, H.; Jerusalem, G. Triple-negative breast cancer: Treatment challenges and solutions. *Breast Cancer* **2016**, *8*, 93–107.
9. Morris, G.J.; Naidu, S.; Topham, A.; McCue, P.; Schwartz, G.; Rosenberg, A.; Mitchell, E.P. Differences in breast carcinoma characteristics in newly diagnosed African-American and Caucasian patients: A single-institution compilation compared with the national cancer institute SEER database. *Cancer* **2007**, *110*, 876–884. [[CrossRef](#)]
10. Denkert, C.; Liedtke, C.; Tutt, A.; Minckwitz, G. Molecular alterations in triple-negative breast cancer—the road to new treatment strategies. *Lancet* **2017**, *389*, 2430–2442. [[CrossRef](#)]
11. Liedtke, C.; Mazouni, C.; Hess, K.R.; Andre, F.; Tordai, A.; Mejia, J.A.; Symmans, W.F.; Gonzalez-Angulo, A.M.; Hennessy, B.; Green, M.; et al. Response to neoadjuvant therapy and long-term survival in patients with triple-negative breast cancer. *J. Clin. Oncol.* **2008**, *26*, 1275–1281. [[CrossRef](#)]
12. Xu, T.; Wang, W.; Zhang, S.; Stewart, R.A.; Yu, W. Identifying tumor suppressors in genetic mosaics: The Drosophila lats gene encodes a putative protein kinase. *Development* **1995**, *121*, 1053–1063. [[CrossRef](#)]
13. Wu, L.; Yang, X. Targeting the Hippo Pathway for Breast Cancer Therapy. *Cancers* **2018**, *10*, 422. [[CrossRef](#)] [[PubMed](#)]
14. Halder, G.; Johnson, R.L. Hippo signaling: Growth control and beyond. *Development* **2011**, *138*, 9–22. [[CrossRef](#)] [[PubMed](#)]
15. Liu, C.; Zha, Z.; Zhou, X.; Zhang, H.; Huang, W.; Zhao, D.; Li, T.; Chan, S.W.; Lim, C.J.; Hong, W.; et al. The Hippo tumor pathway promotes TAZ degradation by phosphorylating a phosphodegron and recruiting the SCF β -TrCP E3 ligase. *J. Biol. Chem.* **2010**, *285*, 37159–37169. [[CrossRef](#)]
16. Zhao, B.; Li, L.; Tumaneng, K.; Wang, C.; Guan, K. A coordinated phosphorylating by LATS and CK1 regulates YAP stability through SCF β -TrCP. *Genes. Dev.* **2010**, *24*, 72–85. [[CrossRef](#)] [[PubMed](#)]
17. Yu, F.X.; Guan, K.L. The Hippo pathway: Regulators and regulations. *Genes. Dev.* **2013**, *27*, 355–371. [[CrossRef](#)] [[PubMed](#)]
18. Holden, J.K.; Cunningham, C.N. Targeting the Hippo pathway and cancer through the TEAD family of transcription factors. *Cancers* **2018**, *10*, 81. [[CrossRef](#)] [[PubMed](#)]

19. Zhao, B.; Ye, X.; Yu, J.; Li, L.; Li, W.; Li, S.; Yu, J.; Lin, J.D.; Wang, C.; Chinnaiyan, A.M.; et al. TEAD mediates YAP-dependent gene induction and growth control. *Genes. Dev.* **2008**, *22*, 1962–1971. [[CrossRef](#)]
20. Lai, D.; Ho, K.C.; Hao, Y.; Yang, X. Taxol resistance in breast cancer cells is mediated by the hippo pathway component TAZ and its downstream transcriptional targets Cyr61 and CTGF. *Cancer Res.* **2011**, *71*, 2728–2738. [[CrossRef](#)]
21. Zhou, Z. Targeting Hippo pathway by specific interruption of YAP-TEAD interaction using cyclic YAP-like peptides. *FASEB J.* **2015**, *29*, 724–732. [[CrossRef](#)]
22. Hilman, D.; Gat, U. The evolutionary history of YAP and the Hippo/YAP pathway. *Mol. Biol. Evol.* **2011**, *28*, 2403–2417. [[CrossRef](#)]
23. Cordenonsi, M.; Zanconato, F.; Azzolin, L.; Forcato, M.; Rosato, A.; Frasson, C.; Inui, M.; Montagner, M.; Parenti, A.R.; Poletti, A.; et al. The Hippo transducer TAZ confers cancer stem cell-related traits on breast cancer cells. *Cell* **2011**, *147*, 759–772. [[CrossRef](#)] [[PubMed](#)]
24. Calvo, F.; Ege, N.; Grande-Garcia, A.; Hooper, S.; Jenkins, R.P.; Chaudhry, S.I.; Harrington, K.; Williamson, P.; Moeendarbary, E.; Charras, G.; et al. Mechanotransduction and YAP-dependent matrix remodelling is required for the generation and maintenance of cancer-associated fibroblasts. *Nat. Cell Biol.* **2013**, *15*, 637–646. [[CrossRef](#)] [[PubMed](#)]
25. Overholtzer, M.; Zhang, J.; Smolen, G.A.; Haber, D.A. Transforming properties of YAP, a candidate oncogene on the chromosome 11q22 amplicon. *Proc. Natl. Acad. Sci. USA* **2006**, *103*, 12405–12410. [[CrossRef](#)] [[PubMed](#)]
26. Chan, S.W.; Lim, C.J.; Guo, K.; Ng, C.P.; Lee, I.; Hunziker, W.; Zeng, Q.; Hong, W. A role for TAZ in migration, invasion, and tumorigenesis of breast cancer cells. *Cancer Res.* **2008**, *68*, 2592–2598. [[CrossRef](#)]
27. Díaz-Martín, J.; López-García, M.Á.; Romero-Pérez, L.; Atienza-Amores, M.R.; Pecero, M.L.; Castilla, M.Á.; Biscuola, M.; Santón, A.; Palacios, J. Nuclear TAZ expression associates with the triple-negative phenotype in breast cancer. *Endocr. Relat. Cancer* **2015**, *22*, 443–454. [[CrossRef](#)]
28. Zhao, D.; Zhi, X.; Zhou, Z.; Chen, C. TAZ antagonizes the WWP1-mediated KLF5 degradation and promotes breast cell proliferation and tumorigenesis. *Carcinogenesis* **2012**, *33*, 59–67. [[CrossRef](#)]
29. Hiemer, S.E.; Szymaniak, A.D.; Varelas, X. The transcriptional regulators TAZ and YAP direct transforming growth factor β -induced tumorigenic phenotypes in breast cancer cells. *J. Biol. Chem.* **2014**, *289*, 13461–13474. [[CrossRef](#)]
30. Nouri, K.; Azad, T.; Ling, M.; Van Rensburg, H.J.J.; Pipchuk, A.; Shen, H.; Hao, Y.; Zhang, J.; Yang, X. Identification of Celastrol as a novel YAP-TEAD inhibitor for cancer therapy by high throughput screening with ultrasensitive YAP/TAZ-TEAD biosensors. *Cancers* **2019**, *11*, 1596. [[CrossRef](#)]
31. Azad, T.; Nouri, K.; Van Rensburg, H.J.J.; Hao, Y.; Yang, X. Monitoring Hippo signaling pathway activity using a luciferase-based large tumor suppressor (LATS) biosensor. *J. Vis. Exp.* **2018**, *139*, e58416.
32. Azad, T.; Van Rensburg, H.J.J.; Lightbody, E.D.; Neveu, B.; Champagne, A.; Ghaffari, A.; Kay, V.R.; Hao, Y.; Shen, H.; Yeung, B.; et al. A LATS biosensor screen identifies VEGFR as a regulator of the Hippo pathway in angiogenesis. *Nat. Commun.* **2018**, *9*, 1061. [[CrossRef](#)]
33. Nouri, K.; Azad, T.; Lightbody, E.; Khanal, P.; Nicol, C.; Yang, X. A kinome-wide screen using a NanoLuc LATS luminescent biosensor identifies ALK as a novel regulator of the Hippo pathway in tumorigenesis and immune evasion. *FASEB J.* **2019**, *33*, 12487–12499. [[CrossRef](#)] [[PubMed](#)]
34. Azad, T.; Tashakor, A.; Hosseinkhani, S. Split-luciferase complementary assay: Applications, recent developments, and future perspectives. *Anal. Bioanal. Chem.* **2014**, *406*, 5541–5560. [[CrossRef](#)] [[PubMed](#)]
35. Adams, S.T., Jr.; Miller, S.C. Beyond D-luciferin: Expanding the scope of bioluminescence imaging in vivo. *Curr. Opin. Chem. Biol.* **2014**, *21*, 112–120. [[CrossRef](#)] [[PubMed](#)]
36. Hall, M.P.; Unch, J.; Binkowski, B.F.; Valley, M.P.; Butler, B.L.; Wood, M.G.; Otto, P.; Zimmerman, K.; Vidugiris, G.; Machleidt, T.; et al. Engineered luciferase reporter from a deep sea shrimp utilizing a novel imidazopyrazinone substrate. *ACS Chem. Biol.* **2017**, *7*, 1848–1857. [[CrossRef](#)]
37. England, C.G.; Ehlerding, E.B.; Cai, W. NanoLuc: A small luciferase is brightening up the field of bioluminescence. *Bioconjug. Chem.* **2016**, *27*, 1175–1187. [[CrossRef](#)] [[PubMed](#)]
38. Dixon, A.S.; Schwinn, M.K.; Hall, M.P.; Zimmerman, K.; Otto, P.; Lubben, T.H.; Butter, B.L.; Binkowski, B.F.; Machleidt, T.; Kirkland, T.A.; et al. NanoLuc complementation reporter optimized for accurate measurement of protein interactions in cells. *ACS Chem. Biol.* **2016**, *11*, 400–408. [[CrossRef](#)]
39. Oh-hashi, K.; Furuta, E.; Fujimura, K.; Hirata, Y. Application of a novel HiBiT peptide tag for monitoring ATF4 protein expression in Neuro2a cells. *Biochem. Biophys. Rep.* **2017**, *12*, 40–45. [[CrossRef](#)]
40. Janse Van Rensburg, H.J.; Azad, T.; Ling, M.; Hao, Y.; Snetsinger, B.; Khanal, P.; Minassian, L.M.; Graham, C.H.; Rauh, M.J.; Yang, X. The Hippo pathway component TAZ promotes immune evasion in human cancer through PD-L1. *Cancer Res.* **2018**, *78*, 1457–1470. [[CrossRef](#)]
41. Nouri, K.; Fansa, E.K.; Amin, E.; Dvorsky, R.; Gremer, L.; Willbold, D.; Schmitt, L.; Timson, D.J.; Ahmadian, M.R. IQGAP1 interaction with RHO family proteins revisited: Kinetic and equilibrium evidence for multiple distinct binding sites. *J. Biol. Chem.* **2016**, *291*, 26364–26376. [[CrossRef](#)]
42. Zhang, K.; Chang, Y.; Shi, Z.; Han, X.; Han, Y.; Yao, Q.; Hu, Z.; Cui, H.; Zheng, L.; Han, T.; et al. ω -3 PUFAs ameliorate liver fibrosis and inhibit hepatic stellate cells proliferation and activation by promoting YAP/TAZ degradation. *Sci. Rep.* **2016**, *6*, 30029. [[CrossRef](#)]

43. Pizato, N.; Luzete, B.C.; Kiffer, L.F.M.V.; Corrêa, L.H.; Santos, I.O.; Assumpção, J.A.F.; Ito, M.K.; Magalhães, K.G. Omega-3 docosahexaenoic acid induces pyroptosis cell death in triple-negative breast cancer cells. *Sci. Rep.* **2018**, *8*, 1952. [[CrossRef](#)]
44. Canadian Cancer Society. Available online: <https://cancer.ca/en/cancer-information/cancer-types/breast/treatment/targeted-therapy> (accessed on 20 December 2022).
45. Ramos, A.; Camargo, F.D. The Hippo signaling pathway and stem cell biology. *Trends Cell Biol.* **2012**, *22*, 339–346. [[CrossRef](#)]
46. Study to Evaluate VT3989 in Patients with Metastatic Solid Tumors Enriched for Tumors with NF2 Gene Mutations. Available online: <https://classic.clinicaltrials.gov/ct2/show/NCT04665206?term=VT3989&draw=2&rank=1> (accessed on 1 July 2023).
47. A Phase I Study of IAG933 in Patients with Advanced Mesothelioma and Other Solid Tumors. Available online: <https://classic.clinicaltrials.gov/ct2/show/NCT04857372?term=IAG933&draw=2&rank=1> (accessed on 1 July 2023).
48. Oral TEAD Inhibitor Targeting the Hippo Pathway in Subjects with Advanced Solid Tumors. Available online: <https://classic.clinicaltrials.gov/ct2/show/NCT05228015> (accessed on 7 July 2023).
49. A Study of ION537 in Patients with Molecularly Selected Advanced Solid Tumors. Available online: <https://classic.clinicaltrials.gov/ct2/show/NCT04659096> (accessed on 7 July 2023).
50. Maity, S.; Gridnev, A.; Misra, J.R. Assays used for discovering small molecule inhibitors of YAP activity in cancers. *Cancers* **2022**, *14*, 1029. [[CrossRef](#)] [[PubMed](#)]
51. Barry, E.R.; Simov, V.; Valtingojer, I.; Venier, O. Recent therapeutic approaches to modulate the Hippo pathway in oncology and regenerative medicine. *Cells* **2021**, *10*, 2715. [[CrossRef](#)] [[PubMed](#)]
52. McCormack, D.; McFadden, D. A review of pterostilbene antioxidant activity and disease modification. *Oxid. Med. Cell. Longev.* **2013**, *2013*, 575482. [[CrossRef](#)] [[PubMed](#)]
53. Wakimoto, R.; Ono, M.; Takeshima, M.; Higuchi, T.; Nakano, S. Differential anticancer activity of pterostilbene against three subtypes of human breast cancer cells. *Anticancer Res.* **2017**, *37*, 6153–6159.
54. Pantziarka, P.; Sukhatme, V.; Crispino, S.; Bouche, G.; Meheus, L.; Sukhatme, P. Repurposing drugs in oncology (ReDO)—Selective PDE5 inhibitors as anti-cancer agents. *Ecancermedicalscience* **2018**, *12*, 824. [[CrossRef](#)]
55. Spano, D.; Marshall, J.C.; Marino, N.; De Martino, D.; Romano, A.; Scoppettuolo, M.N.; Bello, A.M.; Dato, V.D.; Navas, L.; Vita, G.D.; et al. Dipyridamole prevents triple-negative breast-cancer progression. *Clin. Exp. Metastasis* **2013**, *30*, 47–68. [[CrossRef](#)]
56. Tanaka, K.; Osada, H.; Murakami-Tonami, Y.; Horio, Y.; Hida, T.; Sekido, Y. Statin suppresses Hippo pathway-inactivated malignant mesothelioma cells and blocks the YAP/CD44 growth stimulatory axis. *Cancer Lett.* **2017**, *385*, 215–224. [[CrossRef](#)]
57. Sun, S.; Dean, R.; Jia, Q.; Zenova, A.; Zhong, J.; Grayson, C.; Xie, C.; Lindgren, A.; Samra, P.; Sojo, L.; et al. Discovery of XEN445: A potent and selective endothelial lipase inhibitor raises plasma HDL-cholesterol concentration in mice. *Bioorg. Med. Chem.* **2013**, *21*, 7724–7734. [[CrossRef](#)]
58. Han, H.; Qi, R.; Zhou, J.J.; Ta, A.P.; Yang, B.; Nakaoka, H.; Seo, G.; Guan, K.; Luo, R.; Wang, W. Regulation of the Hippo pathway by phosphatidic acid-mediated lipid-protein interaction. *Mol. Cell.* **2018**, *72*, 328–340. [[CrossRef](#)] [[PubMed](#)]

Disclaimer/Publisher's Note: The statements, opinions and data contained in all publications are solely those of the individual author(s) and contributor(s) and not of MDPI and/or the editor(s). MDPI and/or the editor(s) disclaim responsibility for any injury to people or property resulting from any ideas, methods, instructions or products referred to in the content.